ELSEVIER

Biophysical Chemistry 101–102 (2002) 553–564

Biophysical Chemistry

www.elsevier.com/locate/bpc

Temperature jump kinetic study of the stability of apo-calmodulin☆

Carl-Roland Rabl[a], Stephen R. Martin[b], Eberhard Neumann[a], Peter M. Bayley[b,*]

[a]*Faculty of Chemistry, University of Bielefeld, P.O. Box 100130, D-33501 Bielefeld, Germany*
[b]*Division of Physical Biochemistry, National Institute for Medical Research, Mill Hill, London NW7 1AA, UK*

Received 5 February 2002; received in revised form 25 March 2002; accepted 25 March 2002

Abstract

Temperature-jump relaxation spectrometry has been used to study the unfolding properties of Ca^{2+}-free *Drosophila* calmodulin from 278 to 336 K, monitored by absorption of Tyr-138. The T-jump amplitude data are well fitted throughout with a melting temperature $T_m = 315.7$ K, $\Delta H^o_m = 140.5$ kJ mol^{-1} and $\Delta C^o_p = 3.28$ kJ K^{-1} mol^{-1}, giving $\Delta G^o_{293} = 7.36$ kJ mol^{-1} for the C-domain, in good agreement with other data. The relaxation rate observed (time range 1 μs–1 ms) obeys a simple two-state kinetic mechanism throughout. The activation energy for unfolding is nearly temperature-independent, in contrast to that for refolding, and hence the transition state is relatively compact, resembling the folded state, and the relaxation time, τ, shows complex temperature dependence. The domain unfolding is a two-state process occurring with τ of ~100 μs at the T_m. At 296 K, when the C-domain is ~6% unfolded, $k_{unfolding} \approx 305$ s^{-1}, $k_{refolding} \approx 4660$ s^{-1} and $\tau \approx 200$ μs. This closely resembles the rate and extent of a reported C-domain exchange process, inferred from NMR line-broadening at 296 K. The inherent instability of the apo-C-domain of calmodulin indicates that the unfolded form significantly contributes to the physical properties of apo-calmodulin at normal temperatures, and this instability is enhanced by low ionic strength conditions.
© 2002 Elsevier Science B.V. All rights reserved.

Keywords: Calmodulin; Protein folding; Protein dynamics; Relaxation kinetics; Temperature (T)-jump

☆ It is a great pleasure to participate in this Festschrift for John Schellman, who has made so many long-lasting contributions to biophysics and biophysical chemistry. They demonstrate his widely recognised mastery of the subject over a long period of time, and they continue to speak for themselves to a diverse audience. For one of us (P.M.B.) John was a wonderful host in both a scientific and personal sense in post-doctoral days in Eugene. The kindness shown by John and Charlotte Schellman influenced generations of people at all stages of their careers, both inside the laboratory and in the scientific community at large. Working with John, one experienced the inspired style of his approach as a researcher and teacher, exemplified in his consistent search for simplicity of scientific concept and clarity of expression. Over many years, he has been instrumental in helping to establish what we recognise today as the special combination of physical rigour with biological intuition which constitutes the subject of biophysics. If the Schellmans have a motto, it should be: 'Keep it simple, but remember, there are no short cuts!' Thank you, John!

*Corresponding author. Tel.: +44-208-959-3666; fax: +44-208-906-4477.
E-mail address: pbayley@nimr.mrc.ac.uk (P.M. Bayley).

0301-4622/02/$ - see front matter © 2002 Elsevier Science B.V. All rights reserved.
PII: S0301-4622(02)00150-3

1. Introduction

This paper reports new experimental work on the thermal stability of the important eukaryotic protein, calmodulin (CaM). Protein stability studies have a direct link to the formative work of the Schellman laboratory of the 1960s, when the field was in its infancy. The subject has now been transformed by the current capabilities for protein expression, molecular genetics, site-directed mutagenesis and protein engineering, posing even more detailed questions of protein folding mechanisms. The native state of a globular protein, on which biological specificity and selectivity depends, is typically a dynamic structure with only marginal thermodynamic stability. Experimental studies of protein folding processes continue to illuminate the subtle relationship between protein structure and stability.

Calmodulin is a 148-residue protein comprising two structurally distinct domains, (N-domain, residues 1–77; C-domain, residues 78–148) (see [1] for a review). Each domain contains two EF-hands. These segments are formed of a helix–loop–helix motif, with a Ca^{2+}-binding site comprising a sequence of 12 residues, the first 10 of which constitute the loop portion. CaM is best known as the ubiquitous intracellular receptor for Ca^{2+} with which it forms the Ca_4–CaM complex, which in turn acts as the activator of numerous enzymes. The function of Ca^{2+} binding in CaM is to induce a substantial conformational change in both domains, due to the inclusion in the seven-coordinate liganding sphere of the calcium ion, of a bidentate glutamate residue, the 12th and last residue of the Ca^{2+}-binding loop central to the EF-hand helix–loop–helix motif. Conformational changes are essential to target recognition and Ca^{2+}-dependent enzyme regulation by CaM [2]. In addition, CaM acts, apparently in the apo-state, as the 'light chain' for numerous unconventional (i.e. non-muscle) myosins, and the IQ target sequence has now been recognised in a wide range of proteins [3].

Calmodulin is an abundant protein, readily isolated from natural sources, and also expressed in recombinant form; the protein and its mutants have been the subject of numerous biophysical studies of its structure by X-ray crystallography, NMR and optical spectroscopy [1]. The X-ray studies are restricted to structures involving holo-CaM, since to date the apo-form has not been suitably crystallised. As a modular protein of two highly homologous, but distinct structural domains, CaM is of unusual interest for protein folding studies. A primary objective of such studies has been to determine the course of the transition between the native (N) and unfolded (U) states, with particular interest in the definition of 'autonomous folding units' [4] and, by implication, the possible involvement of one or more intermediate states and their relationship to states N or U. Such intermediates may occur either as equilibrium species, or as transient kinetic species, with important implications for the initial steps of either the unfolding of the native protein, or the refolding of the unfolded state. The thermal denaturation of numerous small proteins, such as phageT4 lysozyme [5], shows simple two-state unfolding [6,7], and chemical denaturation has been widely treated from both equilibrium and kinetic perspectives [8–10].

Equilibrium unfolding properties of apo-CaM and its separate apo-domains have recently been studied by thermal and chemical denaturation ([11] and references therein). The interpretation of chemical denaturation data depends on the extrapolation of the experimentally determined free energy of stabilisation as a function of denaturant concentration. The justification for a linear extrapolation of $\Delta G^{o}_{298,[\text{denaturant}]}$ vs. [denaturant], an essential assumption in the analysis, was provided by Schellman [12]. Since the two domains are strongly homologous and structurally similar, apo-CaM provides an interesting model for unfolding studies. The equilibrium unfolding of apo-CaM by chemical denaturation can be resolved into two processes, corresponding to the individual domains, identified using different near- and far-UV optical parameters [11]. The separated apo-C-domain ($\Delta G^{o}_{293} \approx 8.5$ kJ mol^{-1}) is less stable than the apo-N-domain ($\Delta G^{o}_{293} \approx 12.5$ kJ mol^{-1}), and in the intact apo-CaM, the C-domain is further destabilised by ~ 2.7 kJ mol^{-1}, while the N-domain is stabilised by a similar amount.

The same effects are observed in thermal stability: the T_m of the C-domain in intact apo-CaM

(43.5 °C) is lower than the separate C-domain (49.4 °C), whereas the T_m of the N-domain in intact apo-CaM (57.5 °C) is increased relative to the separate N-domain (50.3 °C). Thus the T_m values of the separate domains are closely similar, and the resolvable difference in intact apo-CaM appears to be due to the interaction of the unfolded C-domain with the (folded) N-domain. The total free energy of stabilisation of either apo-domain is small, consistent with the treatment of protein thermal stability given by Becktel and Schellman [7], also rationalising the fact that point mutations can cause remarkable changes in T_m for both domains [13]. The effect of Ca^{2+} binding on stability follows the predictions of the ligand binding theory as described by Schellman [14], with the stability of the C-domain (having higher affinity for Ca^{2+} than the N-domain) being more sensitive to Ca^{2+} binding. By contrast, Mg^{2+} has greater affinity for the N-domain [15], and may have the function of exerting some protective effect on CaM when intracellular $[Ca^{2+}]$ is low (<100 nM).

Measurements of the stability of the C-domain of apo-CaM [11] showed that this domain is partially unfolded at room temperature. This would have relevance to many biophysical studies, for example optical and especially NMR spectroscopy, on which the current structural model of apo-CaM and its domains is based [16–18]. The line-broadening of apo-C-domain NMR resonance showed that the C-domain was intrinsically more dynamic than the N-domain on a sub-ms time-scale [19]. In addition, many of the intra-strand NOE effects normally observed in the C-domain disappeared at low ionic strength, presumably due to expansion of the highly negatively charged domain [20]. Consistent with this, the thermal and chemical denaturation of apo-CaM (and its individual domains) have been shown to be significantly enhanced at low ionic strength [11], but they are largely unaffected by pH in the range 6–8, covering typical conditions of both optical and NMR experiments.

By contrast with the detailed equilibrium description, less is known in quantitative terms about the kinetics of the dynamic processes and the possible existence of transient kinetic intermediates. Currently, the most widely used experimental approach to folding kinetics is to initiate a denaturant concentration relaxation process by stopped-flow mixing, and observing either Trp-fluorescence or (less commonly) peptide circular dichroism (CD). (In fact, stopped-flow CD, reviewed in [21], also owes a debt to John Schellman's encouragement.) The refolding process from guanidine hydrochloride of parvalbumin, a CaM-related EF-hand protein, occurred within the 18-ms dead time of the far-UV CD stopped-flow apparatus [22]. The limitations in time resolution may be overcome in due course by new mixing techniques [23]. However, shorter time-resolution can be obtained with the well-established technique of temperature-jump relaxation, pioneered by Eigen and co-workers [24]. This technique is widely applicable for proteins in an essentially physiological buffer. It involves observation of temperature-induced perturbations of a balanced equilibrium system as a function of temperature, with fluorescence or absorption measurements at μs time resolution. Sub-μs resolution is now available through laser-induced T-jump [25]. The related technique of pressure jump, either in single-shot or repetitive mode, offers analogous information, with time resolution of 50 μs and longer [26]. The kinetic approach to studying protein stability using relaxation techniques does not appear to have been applied to CaM or its homologues.

The stability of both domains of CaM is increased by Ca^{2+} binding [11,27], to an extent determined by the calcium concentration (cf. [14]). Thus, it is the stability of the apo-form that is central to the thermodynamic properties of the system. The aim of the present work was to characterise both the equilibrium and kinetics of the complete unfolding transition of the C-domain of apo-CaM as a function of temperature, monitored by the absorption of the single Tyr-138 of *Drosophila* CaM. We report refinements of the T-jump technique applied over a 60 °C temperature range. The data analysis has been extended to examine critically the possible role of kinetic intermediate species in this reaction, in order to establish the consistency of the kinetic model with that deriving from equilibrium studies. The kinetic

approach provides additional thermodynamic criteria that help to define the complexity and the time range of the structural relaxation of apo-CaM C-domain.

2. Materials and methods

Drosophila CaM was expressed in *E. coli* and purified as described elsewhere [13]. Calcium-free (apo) samples were prepared by incubating with 5–25 mM EGTA and then desalting by passage though two Pharmacia PD10 (G25) columns equilibrated with Chelex-treated buffer (25 mM Hepes, 100 mM KCl, pH 7.5). All measurements were made with apo-CaM (240 μM) in 25 mM Hepes, 100 mM KCl, 1 mM EDTA (pH 7.5). In order to avoid bubbles and cavitation at high temperatures, the samples were carefully degassed prior to all measurements. Solvent loss was avoided by using a closed degassing syringe.

Static melting curves were measured with a Uvikon 930 spectrophotometer (Kontron, Eching, Germany) using a bandwidth of 1 nm and an integration time of 4 s. Fused silica cuvettes (10×10 mm^2) were closed with a PTFE plug to prevent solvent loss at high temperature. Solutions were heated at 30 K h^{-1} using a modified K4R kryothermostat (Messgeraete-Werk Lauda/Tauber, Germany). The temperature was measured using a digital thermometer (TDA-01, Telemeter Electronic, Donauwoerth/Germany) with a Pt-1000 temperature sensor in one corner of the cuvette. Uniform thermostatting was achieved using a rapidly spinning PTFE magnet, controlled by a Varimag electronic mini-stirrer (H+P-Apparatebau, Munich, Germany). The error in the temperature was $\leq$0.2 K.

T-jump measurements were made using a modified version of the instrument described by Rigler et al. [28]. It is equipped for measurements of both absorption and fluorescence, and was manufactured by Dia-Log GmbH (Düsseldorf, Germany). The light source (200-W Hg/Xe lamp; Hanovia 901 B 11) gives a very intense line spectrum of Hg with a small, continuous background of Xe, but has a stability very similar to a pure Xe-lamp. The monochromator is the high-intensity Schoeffel GM 250 (250 mm, grating 1180 lines mm^{-1} blazed at 300 nm, aperture 1:3.4). The original photomultiplier heads in the absorption and reference light path were replaced by photodiode heads (UV-Vis silicon photodiodes, RCA C 30839) [29,30]. The T-jump sample cell was the high-temperature design described in Appendix A. The T-jump monochromator was set to a bandwidth of 10 nm in order to obtain enough light for low-noise signals in the μs-range (bandwidth defined by 50%-points). The static wavelength was selected with respect to a doublet line of neutral Hg(I) at 280.4 nm. Careful reinspection revealed that there were also spectral lines at 281.5 and 284.8 nm from ionised Hg(II). The optical density of Tyr-138 strongly decreases above 280 nm [31]. Thus, the effective T-jump wavelength was approximately 283 nm and the T-jump amplitude, after careful calibration of the T-jump cell, was 20% lower than that calculated from the static melting curve at 280.4 nm.

The measurements were made with the temperature linearly increasing at 15 K h^{-1}. T-jumps of 1.2 K were made at 6-min intervals in order to allow time for sufficient thermal re-equilibration between jumps. The upper temperature limit of 336 K was determined by experimental limitations, particularly with cavitation. Most T-jumps were made with a sampling time of 1 μs and a total time axis of 16 ms. No relaxation processes were found at longer times. The electronic rise-time filter constant was either 2 or 5 μs. The sample conductance was 4 mS at 278 K and 2.5-fold greater at 336 K; thus, the heating-energy time constant was 1–6 μs with charge capacitors of 20 and 50 nF. The convolution of both time constants gives the effective signal rise time, which has been accounted for in the fitting process. A small, unresolved fast effect present with all T-jumps, due to the thermal expansion of water and the temperature dependence of the extinction coefficients, was subtracted. The relaxation times refer to the final temperature after the T-jump, and the amplitudes to the average of the initial and final temperature.

Data were collected using a Bryans/Physical Data 523A transient recorder (10 MHz, 10 bit, dual time base), and analysed using a multi-exponential fitting program based on a modified

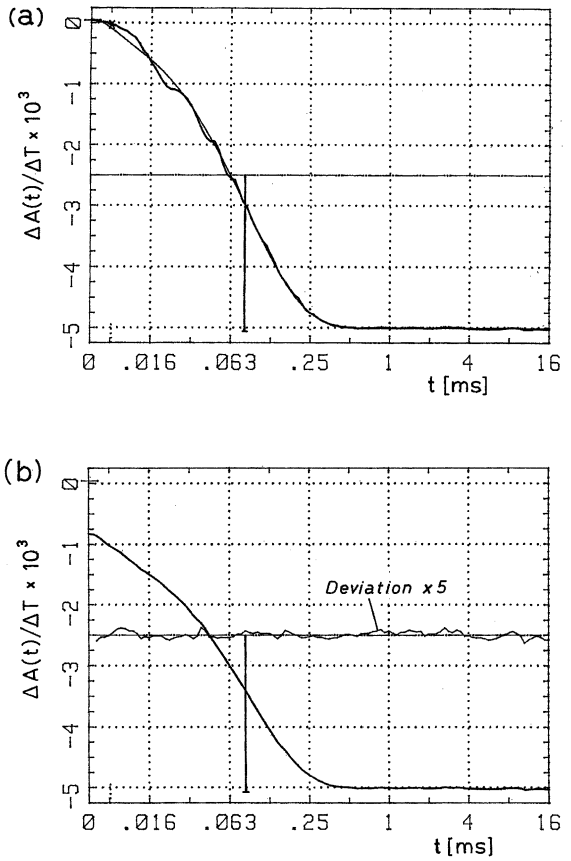

Fig. 1. T-jump relaxation of 240 μM apo-CaM (final temperature 317.8 K) plotted on a quasi-log time axis (see text). The amplitude axis has been normalised to $\Delta T = 1$ K and a 10-mm optical path length. Signal rise time 5.6 μs, relaxation time 83 μs (indicated by the vertical bar). (a) Original measurement with fit (*thin line*). (b) As curve (a), but digitally filtered with time shifts $t_1 = 29$ μs and $t_2 = 9$ μs to suppress pressure oscillations. The residual fitting error around the centre line is enlarged five-fold.

Marquardt algorithm. The relaxation curves were plotted on a quasi-log time axis, in which the first 15 data points have a linear time scale, followed by a log time axis with 10 data points per time interval 1:2 (see Fig. 1, which shows the T-jump relaxation of 240 μM apo-CaM for a final temperature 317.8 K). Thus, 116 data points span a time interval of 1:16 000. The slope of the curves is continuous at the linear/log switching point. The implied data-reduction algorithm gives an excellent compromise between data resolution and noise reduction. The data points given in the figures are for individual T-jumps.

Additional information could be obtained using Tyr-138 fluorescence measurements. Static fluorescence measurements show a fairly broad transition, with increasing fluorescence intensity near to 315 K, superimposed on thermal quenching. Fluorescence T-jump measurements [excitation at 283 nm; emission through long pass filter (Schott WG 320)] show an unresolved fast decrease due to the thermal quenching followed by a time-resolved increase, which is compatible with the absorption measurements. These fluorescence signals are, however, noisier than the absorption signals and were not used in the analysis.

A two-state unfolding/refolding reaction of a protein is formulated as:

$$\mathrm{N} \underset{k_\mathrm{N}}{\overset{k_\mathrm{U}}{\rightleftharpoons}} \mathrm{U} \tag{1}$$

where k_U and k_N are the rate coefficients for unfolding and refolding, respectively. The equilibrium constant K is the concentration ratio $c_\mathrm{U}/c_\mathrm{N}$, which is:

$$K = c_\mathrm{U}/c_\mathrm{N} = k_\mathrm{U}/k_\mathrm{N} = \exp\left[-\Delta G^\mathrm{o}(T)/RT\right] \tag{2}$$

$$\Delta G^\mathrm{o}(T) = \Delta H^\mathrm{o}(T) - T \cdot \Delta S^\mathrm{o}(T) \tag{3}$$

where $\Delta G^\mathrm{o}(T)$, $\Delta H^\mathrm{o}(T)$, and $\Delta S^\mathrm{o}(T)$ are the standard values of the Gibbs energy, the enthalpy and the entropy, respectively. The temperature dependence of $\Delta H^\mathrm{o}(T)$ and $\Delta S^\mathrm{o}(T)$, and thus of $\Delta G^\mathrm{o}(T)$, is expressed as:

$$\Delta H^\mathrm{o}(T) = \Delta H^\mathrm{o}_\mathrm{m} + \Delta C^\mathrm{o}_\mathrm{p}(T - T_\mathrm{m}) \tag{4}$$

$$\Delta S^\mathrm{o}(T) = \Delta S^\mathrm{o}_\mathrm{m} + \Delta C^\mathrm{o}_\mathrm{p} \cdot \ln(T/T_\mathrm{m}) \tag{5}$$

where the subscript m denotes values at the melting temperature T_m (where $K = 1$). $\Delta C\mathrm{p}^\mathrm{o} = C^\mathrm{o}_\mathrm{U} - C^\mathrm{o}_\mathrm{N}$ is the heat capacity change between states U and N. Substituting $\Delta S^\mathrm{o}_\mathrm{m} = \Delta H^\mathrm{o}_\mathrm{m}/T_\mathrm{m}$ yields:

$$\Delta G^\mathrm{o}(T) = \Delta H^\mathrm{o}_\mathrm{m}(1 - T/T_\mathrm{m}) + \Delta C^\mathrm{o}_\mathrm{p}\left[T - T_\mathrm{m} - T \cdot \ln(T/T_\mathrm{m})\right] \tag{6}$$

In studying protein unfolding using optical measurements, we must allow for the fact that the extinction coefficients ε_N and ε_U depend slightly

on temperature:

$$\varepsilon_i(T) = \varepsilon_{i,\mathrm{m}} + \varepsilon'_i(T - T_\mathrm{m}) \quad i = \mathrm{U,N} \tag{7}$$

If the total protein concentration is written as $c_0 = c_\mathrm{N} + c_\mathrm{U}$, the absorbance per unit length is:

$$\begin{aligned} A(T) &= \varepsilon_\mathrm{N}(T)c_\mathrm{N} + \varepsilon_\mathrm{U}(T)c_\mathrm{U} \\ &= \left\{\varepsilon_\mathrm{N}(T) + \left[\varepsilon_\mathrm{U}(T) - \varepsilon_\mathrm{N}(T)\right]\cdot K/(1+K)\right\}c_0 \end{aligned} \tag{8}$$

where $c_\mathrm{U}/c_0 = K/(1+K)$ is the degree of conversion. The fit to this equation (using GRAFIT 3) yields the static data set: T_m, $\Delta H^\mathrm{o}_\mathrm{m}$, $\Delta C^\mathrm{o}_\mathrm{p}$, $\varepsilon_{\mathrm{N,m}}$ and $\varepsilon_{\mathrm{U,m}}$. Values of ε'_N and ε'_U were estimated from the data at low and high temperatures.

The T-jump amplitude is obtained by differentiating Eq. (8) and multiplying by the temperature jump ΔT. There is a small, instantaneous, fast component due to the temperature-dependent extinction coefficients:

$$\begin{aligned} \Delta A(T)_\mathrm{fast} = &\left[\varepsilon'_\mathrm{N}\right. \\ &\left. + (\varepsilon'_\mathrm{U} - \varepsilon'_\mathrm{N})\cdot K/(1+K)\right]c_0\Delta T \end{aligned} \tag{9}$$

The time-resolved kinetic amplitude is analysed using:

$$\begin{aligned} \Delta A(T)_\mathrm{kin} = &\left[\varepsilon_\mathrm{U}(T) - \varepsilon_\mathrm{N}(T)\right]\cdot\left[K/(1+K)^2\right] \\ &\cdot\left[\Delta H^\mathrm{o}(T)/RT^2\right]\cdot c_0\Delta T \end{aligned} \tag{10}$$

to yield the kinetic data set: T_m, $\Delta H^\mathrm{o}_\mathrm{m}$, $\Delta C^\mathrm{o}_\mathrm{p}$ and $\varepsilon_{\mathrm{U,m}} - \varepsilon_{\mathrm{N,m}}$.

For a two-state unfolding reaction, the reciprocal relaxation time is equal to the sum of the rate coefficients k_U and k_N for unfolding and refolding:

$$1/\tau = k_\mathrm{U} + k_\mathrm{N} = (1 + 1/K)k_\mathrm{U} = (1+K)k_\mathrm{N} \tag{11}$$

The rate coefficients are related to the activation energies $E_{\mathrm{a,U}}$ and $E_{\mathrm{a,N}}$ and to the activation entropies $S_{\mathrm{a,U}}$ and $S_{\mathrm{a,N}}$ by:

$$k_i = \exp\left[-E_{\mathrm{a},i}(T)/RT + S_{\mathrm{a},i}(T)/RT\right] \quad i = \mathrm{U,N} \tag{12}$$

We assume that $\Delta H^\mathrm{o}(T) = E_{\mathrm{a,U}}(T) - E_{\mathrm{a,N}}(T)$ and $\Delta S^\mathrm{o}(T) = S_{\mathrm{a,U}}(T) - S_{\mathrm{a,N}}(T)$. Therefore, analogous to Eq. (4) and Eq. (5):

$$E_{\mathrm{a},i}(T) = E_{\mathrm{am},i} + C_{\mathrm{a},i}(T - T_\mathrm{m}),$$

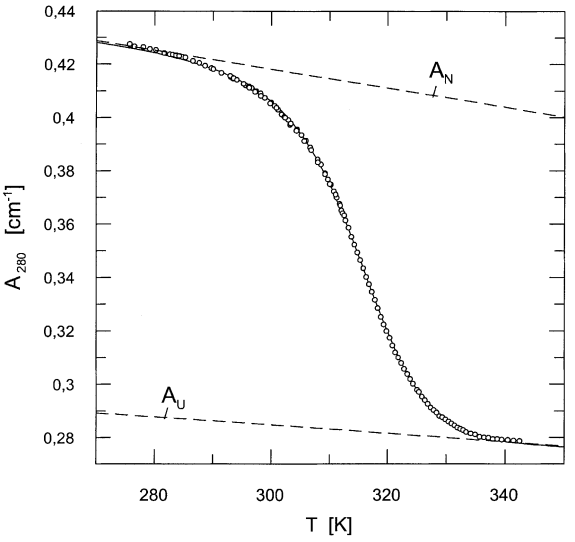

Fig. 2. Static melting curve for 240 μM apo-CaM measured at 280.4 nm. The solid line is the computed best fit to Eq. (8).

$$S_{\mathrm{a},i}(T) = S_{\mathrm{am},i} + C_{\mathrm{a},i}\cdot\ln\left(T/T_\mathrm{m}\right), \qquad i = \mathrm{U,N} \tag{13}$$

where $C_{\mathrm{a},i}$ is the heat capacity of activation. With respect to the numerical analysis, we define k_m as the rate coefficient for unfolding *and* refolding at $T = T_\mathrm{m}$. Substituting $k_\mathrm{m} = \exp(-E_{\mathrm{am},i}/RT_\mathrm{m} + S_{\mathrm{am},i}/R)$ yields:

$$\begin{aligned} k_i = k_\mathrm{m}\exp\Big\{ &-E_{\mathrm{am},i}(1 - T/T_\mathrm{m})/ \\ &RT - C_{\mathrm{a},i}\left[T - T_\mathrm{m} - T\cdot\ln\left(T/T_\mathrm{m}\right)\right]/RT\Big\}, \\ &i = \mathrm{U,N} \end{aligned} \tag{14}$$

Combining Eq. (11) and Eq. (14) and using K and T_m calculated from the time-resolved amplitude data, the fit of $1/\tau$ yields k_m, $E_{\mathrm{am,U}}$ and $C_{\mathrm{a,U}}$. The corresponding quantities for the refolding reaction are $E_{\mathrm{am,N}} = E_{\mathrm{am,U}} - \Delta H^\mathrm{o}_\mathrm{m}$ and $C_{\mathrm{a,N}} = C_{\mathrm{a,U}} - \Delta C^\mathrm{o}_\mathrm{p}$. The solid lines in the Arrhenius plots are then easily calculated. The individual rate coefficients at any temperature are calculated as $k_\mathrm{N} = (1/\tau)/(1+K)$ and $k_\mathrm{U} = (1/\tau)/(1+1/K)$.

3. Results and discussion

Analysis of the static (equilibrium) absorbance data (Fig. 2) and the T-jump amplitude data (Fig. 3) show that the thermal unfolding process moni-

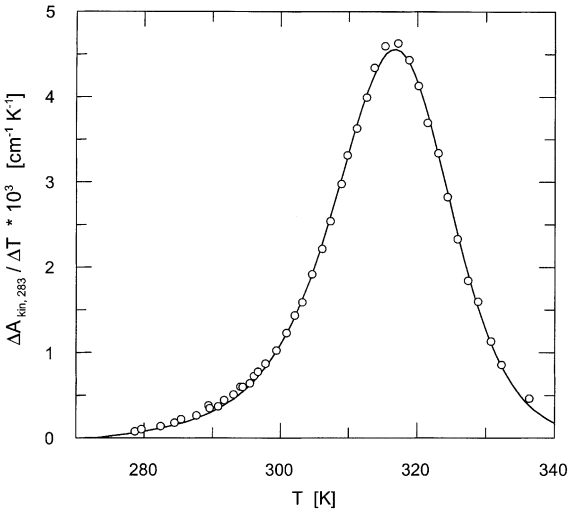

Fig. 3. Normalised T-jump amplitude for 240 μM apo-CaM measured at 283 nm. The solid line is the computed best fit to Eq. (10).

tored here using Tyr-138 is well accounted for in terms of a simple two-state unfolding equilibrium. Values of ΔH^{o}_{m}, T_m and ΔC^{o}_{p} determined from these two analyses are in excellent agreement (Table 1) and are closely similar to published values determined under slightly different solvent conditions [11,32]. Although only the signal from the single tyrosine residue is monitored in this study, the thermodynamic parameters correspond well to those determined for the C-domain by monitoring thermal unfolding using the change in its overall secondary structure, as assessed by far-UV CD [11]. We also note that the ΔC^{o}_{p} value (3.28 kJ K^{-1} mol^{-1}), the calculated ΔH^{o}_{333} value (197 kJ mol^{-1}) and the calculated ΔS^{o}_{333} value (0.62 kJ K^{-1} mol^{-1}) are very similar to those predicted for a protein with 71 residues (4.11 kJ K^{-1} mol^{-1}, 210 kJ mol^{-1} and 0.63 kJ K^{-1} mol^{-1}, respectively [33]). The thermodynamic parameters determined here predict a low free energy of stabilisation at 293 K (ΔG^{o}_{293}) of 7.36 kJ mol^{-1}. This value agrees well with the value determined using urea unfolding at this temperature [11], and is consistent with the observation that point mutations in the hydrophobic core (of either domain of CaM) can markedly reduce the stability (with reductions in T_m of more than 50 °C in some

Table 1
Thermodynamic parameters for unfolding of the C-domain in apo-calmodulin

	Static[a] (280.4 nm)	T-jump amplitude (283 nm)
ΔH^{o}_{m} (kJ mol^{-1})	139.1 ± 0.6	140.5 ± 1.3
T_m (K)	315.03 ± 0.03	315.72 ± 0.10
ΔC^{o}_{p} (kJ K^{-1} mol^{-1})	3.357 ± 0.074	3.278 ± 0.23
$\varepsilon_{N,m}$ (M^{-1}·cm^{-1})	1727.4 ± 0.92	–
$\varepsilon_{U,m}$ (M^{-1}·cm^{-1})	1172.2 ± 0.63	–
$\varepsilon_{U,m} - \varepsilon_{N,m}$ (M^{-1}·cm^{-1})	−555.2 ± 1.3	−444.6 ± 3

Tolerances are standard deviations of the multiparameter fitting.

[a] ε'_N and ε'_U were fixed at −1.54 and −0.58 M^{-1} cm^{-1} K^{-1}, respectively, in the analysis of the static data (see text).

cases), and hence cause complete unfolding at normal temperatures [13].

Although the variation in relaxation rate, τ^{-1} ($=k_U+k_N$), with temperature (Fig. 4) is complex, it is also well accounted for by a simple two-state unfolding mechanism. Plots of the individual rate coefficients as log(k) vs. ($1/T$) are not linear for either folding or unfolding (Fig. 5), as expected for a reaction with a heat capacity change between the ground and activated states. The curve for the unfolding rate coefficient (k_U) is, in fact, close to

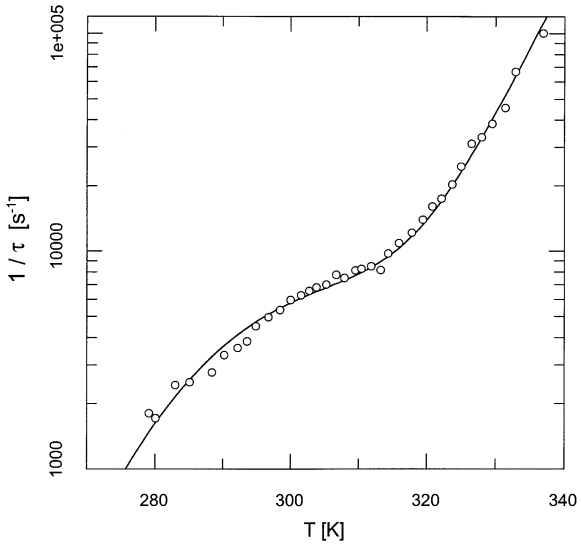

Fig. 4. Variation of the reaction rate τ^{-1} with temperature. The solid line is the computed best fit to Eq. (14).

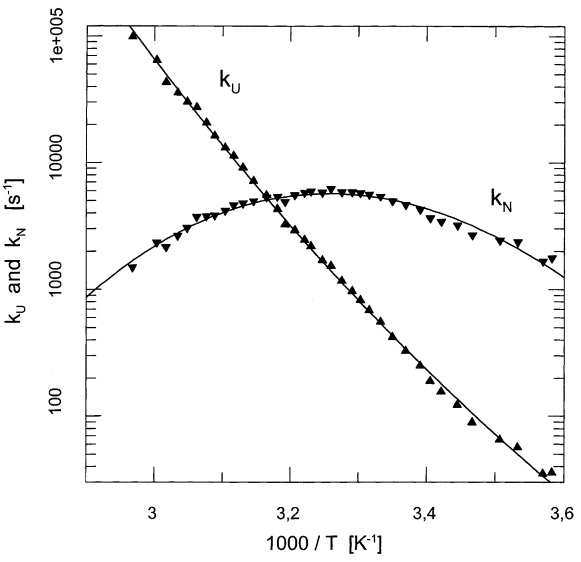

Fig. 5. Variation of the rate coefficients k_U and k_N with temperature. The solid lines were calculated using Eq. (12).

linearity, with the rate coefficient varying by almost four orders of magnitude over the temperature range studied. This is because $E_{am,U}$ is large and positive, and $C_{a,U}$ is small and positive (Table 2). By contrast, the curve for the folding rate coefficient (k_N) shows very high curvature. It goes through a maximum of $\sim 5700\ s^{-1}$ at 307 K and remains within one order of magnitude over the entire temperature range studied. This is because $E_{am,N}$ is small and negative, whilst $C_{a,N}$ is large and negative (Table 2). This characteristic behaviour of the folding rate coefficient has now been reported for a number of small proteins [5,26,34–37], and this breakdown of the total ΔC_p^o (with a small $E_{am,N}$) is taken to indicate the existence of a compact transition state, which maintains most of the hydrophobic interactions of the native state.

4. Conclusions: the dynamics of the apo-CaM C-domain

The biological function of calmodulin requires a potentially dynamic structure to allow for Ca^{2+}-induced conformational changes. Structural disorder of holo-CaM [38] has been analysed in terms of the correlated motion of substructures, potentially implying a continuum of (closely related) structures in solution, which could facilitate target-dependent adjustment of its surfaces to optimise docking interactions. Consistent with this, ^{15}N NMR relaxation measurements [39] show that the backbone dynamics of holo-CaM domains reflect the global motion of a given domain. The NMR studies of apo-CaM show it to be a much more dynamic structure than holo-CaM, with a much greater breadth of conformational distribution. The EF-hand loop sequences are much less structured, and the C-domain specifically shows general line-broadening of many residues. This effect is attributed to exchange processes on the time-scale of 100s of μs, consistent with dynamic exchange between the majority species and ~10% of one or more additional conformers [16,17,19]. The dynamic nature of the apo-state is also illustrated by the observation [20] that, in solutions of low ionic strength, the intra-strand NOE signals of the apo-C-domain disappear, implying (at least) an expansion of the molecule, which carries high negative charge at neutral pH, but with retention of secondary structure. Thus CaM, particularly in its apo-state, is a molecule that exhibits an unusual degree of flexibility, especially in the C-domain. However, the locally dynamic nature of the folded state evidently does not result in additional complexity of the two-state equilibrium unfolding reaction of this domain.

A further feature of the domain structure of CaM relates to a possible interaction of the domains during the unfolding process, [11]. The apo-C-domain is the less stable of the two domains, and will generally unfold in the presence of a folded apo-N-domain. The observation that the thermodynamic stability for the apo-C-domain

Table 2
Kinetics parameters for unfolding of the C-domain in apo-calmodulin

	Unfolding	Refolding
i=U,N	k_U	k_N
k_m (s^{-1})	5090±96	(5090±96)
$E_{am,i}$ (kJ mol^{-1})	119.5±1.1	−21.0±2.0[a]
$C_{a,i}$ (kJ K^{-1} mol^{-1})	0.856±0.090	−2.42±0.3[a]

[a] Including tolerances of amplitude fitting.

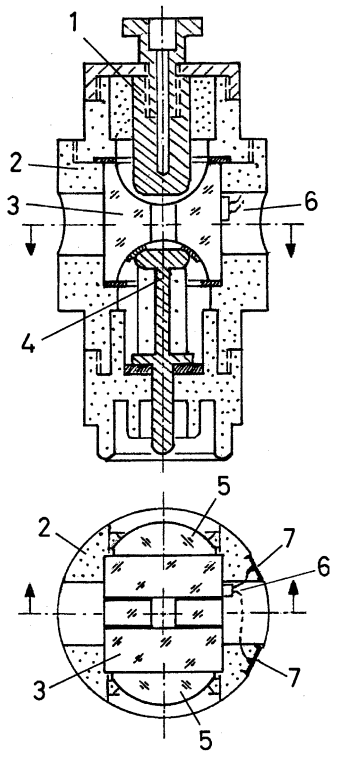

Fig. 6. High-temperature T-jump sample cell: (a) vertical cross-section in the absorption/excitation light path; and (b) horizontal cross-section in the centre of the cell. Coarse hatching, stainless steel and brass; dense hatching, silicon rubber; dotted, plastic (black polyacetal resin, polyurethane foam with lower electrode); clear, fused silica. Electrodes are coated with solid platinum. Numbering: 1, cell head with grounded upper electrode; 2, cell body; 3, fused silica cube with sample cavity; 4, lower electrode with high-voltage connector; 5, plan convex lenses with emission windows; 6, Pt-1000 temperature sensor; and 7, connectors for the Pt-1000 sensor.

of CaM is lower than that of the isolated domain has been interpreted as involving an interaction between the unfolded C-domain and the folded N-domain. This occurs without perturbation of the equilibrium unfolding mechanism, which follows a two-state unfolding process for each domain [11].

The work described here shows that the kinetics of the thermal unfolding of the C-terminal domain of apo-CaM may also be described as a transition between just two states, namely the folded and unfolded forms of the C-domain. The process is therefore kinetically described by the two rate coefficients for folding and unfolding. The absence of any additional kinetic processes in the time range observed (2 μs to ~16 ms, and longer times using the cooling correction described by Rabl [40]) indicates the persistence of this two-state behaviour over the full temperature range studied. There is therefore no evidence for an additional intermediate kinetic state of the C-domain that might be related to a substructural component (e.g. one EF-hand of the pair comprising the domain). The single relaxation process is associated with unfolding of the C-domain in the presence the (predominantly) folded N-domain (see above). Possible minor, coupled relaxation processes, associated for example with the alternative, less probable pathway of the unfolding of the C-domain in the presence of an already unfolded N-domain, would most probably have a similar native-like transition state for the C-domain, and hence a similar unfolding rate (which dominates the relaxation rate at high temperatures). Such a pathway would be expected to contribute more significantly to the data only at high temperatures (>325 K), where amplitudes are small. It is unlikely, therefore, that such a process would be detectable in these experiments as a possible differential relaxation of the C-domain in the presence of either folded or unfolded N-domain. Hence, the two-state kinetic behaviour appears fully consistent with the two-state equilibrium unfolding mechanism for this domain.

The thermodynamic parameters for the C-terminal domain of CaM (Table 1) enable us to calculate that the percentage of molecules with an unfolded C-domain varies from ~2.5% at 10 °C to ~13% at 30 °C under our experimental conditions. The relaxation time for equilibration between the native and unfolded forms $[(k_U+k_N)^{-1}]$ varies from ~470 μs at 10 °C to ~160 μs at 30 °C. Hence, many biophysical measurements on apo-CaM under typical conditions (10–30 °C and 100 mM KCl) are likely to include contributions from both folded and unfolded states of the protein. At lower ionic strengths, where CaM is even less stable [11], the percentage of molecules with an unfolded C-domain is still higher. The biophysical studies detailed in Section 1 [16,17,19,38] illus-

trate the presence in apo-CaM of dynamic processes within either domain, and more evidently in the C-domain. Thus, we can enquire whether these dynamic exchange processes represent unfolding, or are a composite of minor variations in structure of the apo-domain that do not involve large changes in exposed surface area, and hence solvent interaction. These structures would then be effectively isoenergetic, and likely to exchange relatively rapidly. The exchange process identified by NMR is reported to involve approximately 5–10% of an additional state, but is in fact relatively slow, with a relaxation time of a few 100 μs (~350 μs, [19]). This relaxation time is very similar to that for equilibration between the native and unfolded forms of the apo-C-domain, which we calculate to be ~200 μs at the temperature of the NMR experiment (23 °C), where the domain is ~6% unfolded. Hence, both the time scale and the magnitude of the effect appear fully consistent with the NMR properties affected by the kinetics and the extent of the folding–unfolding process. It should be noted that hydrogen exchange at 23 °C shows a large number of rapidly exchanging backbone NH moieties in the C-domain, but also a smaller number of slowly exchanging residues, particularly in helix-G, indicating the persistence of some degree of protection [19]. Thus, while it appears that this unfolded state must retain at least a small amount of residual structure, we conclude that the unfolded state of the apo-C-domain is implicated in the exchange process inferred from the NMR line-broadening observed.

Appendix A: High-temperature T-jump cell

The insulating body of a T-jump cell is made of plastic (e.g. black polyacetal resin). The optical windows are usually cones of high-quality fused silica and the electrodes are cold-drawn gold or platinum, soldered onto brass. The sample cells are inserted into a large, temperature-controlled metal block with a high-voltage (HV) connector at the bottom. Thermal equilibration is mainly achieved via the grounded upper electrode.

Two problems are inherent with plastic material: low thermal conductivity and a large thermal expansion coefficient. The first problem has been partly overcome by armouring black PTFE with stainless steel [28]. This armouring cannot, however, be used over an extended temperature range because of the different thermal expansion, especially with conical wide-angle fluorescence emission windows. The high-temperature cell shown in Fig. 6 was due to an idea of Detlev Riesner (see [41]). The centre part is a hollow cube of fused silica plates with half-spherical cut-outs above and below a sample cavity of 7 mm in path length (manufactured by Hellma, Muellheim, Germany). Some modifications to the original design have been made to reduce sample volume, improve the HV breakdown limit, reduce the thermal inertness (by reducing the thermal mass of the lower electrode) and improve temperature measurement. The distance between the electrodes is 12 mm and the minimum sample volume is 1.3 ml. Differences in the thermal expansion of different materials have been buffered using silicon rubber. The main advantage of the fused silica cube is that the conductivity of heat is five-fold better than that of conventional plastics. A small Pt-1000 thin-film resistor (M-FK 422, Heraeus, Hanau, Germany) is mounted near to the entrance window and connected to a linearised digital-thermometer device with a four-pole connector.

For thermal calibration, the upper electrode has been replaced by a stainless steel electrode of the same dimensions. This electrode had two deep, blind holes and a central through-hole. In one blind hole there is another Pt-1000 element to measure the electrode temperature. In the other two holes, there is a precisely matched pair of NTC-thermistors in a bridge circuit to measure the temperature difference between the electrode and the centre of the liquid sample. The thermistors have a thin shaft (2×25 mm^2) of glass tubing; the position of the thermistor in the liquid is adjusted to be slightly below the centre of the optical axis with respect to the thermal conductivity of the glass shaft. Two other platinum thermometers are used for monitoring the thermostat bath temperature and the cell holder temperature. Thus, there are six points of temperature measurement, and a computer program is used for monitoring the various temperatures and temperature differ-

ences. The electrolytic conductivity of the sample is also monitored.

Increasing the thermostat bath temperature at 18 K h^{-1} increased the temperature rise within the cell at 15 K h^{-1}. The temperature difference between the centre of the cell and the Pt-1000 at the outside of the fused silica cube was ± 0.1 K at 289 K and 0.2 ± 0.3 K at 333 K. The corresponding temperature difference between the upper electrode and the centre of the cell was ± 0.1 K at 289 K and 2.2 ± 0.3 K at 333 K. Referred to the sample volume observed by the light path, the uncertainty of the Pt-1000 reading is less than 1 K, also at lower temperatures.

References

[1] A. Crivici, M. Ikura, Molecular and structural basis of target recognition by calmodulin, Annu. Rev. Biophys. Biomol. Struct. 24 (1995) 85–116.

[2] A.R. Rhoads, F. Friedberg, Sequence motifs for calmodulin recognition, FASEB J. 11 (1997) 331–340.

[3] M. Bähler, A. Rhoads, Calmodulin signalling via the IQ motif', FEBS Lett. 513 (2002) 107–113.

[4] Z.-Y. Peng, L.C. Wu, Autonomous protein folding units, Adv. Protein Chem. 53 (2000) 1–47.

[5] B.-L. Chen, W.A. Baase, J.A. Schellman, Low-temperature unfolding of a mutant of phage T4 lysozyme. 2. Kinetic investigations, Biochemistry 28 (1989) 691–699.

[6] J.A. Schellman, The thermodynamic stability of proteins, Annu. Rev. Biophys. Biophys. Chem. 16 (1987) 115–137.

[7] W.J. Becktel, J.A. Schellman, Protein stability curves, Biopolymers 26 (1987) 1859–1877.

[8] S.E. Jackson, How do small single-domain proteins fold?, Folding Des. 3 (1998) R81–R91.

[9] C.N. Pace, Determination and analysis of urea and guanidine hydrochloride denaturation curves, Methods Enzymol. 131 (1986) 266–280.

[10] R. Fersht, Structure and Mechanism in Protein Science: A Guide to Enzyme Catalysis and Protein Folding, W.H. Freeman, New York, 1998.

[11] L. Masino, S.R. Martin, P.M. Bayley, Ligand binding and thermodynamic stability of a multidomain protein, calmodulin, Protein Sci. 9 (2000) 1519–1529.

[12] J.A. Schellman, Solvent denaturation, Biopolymers 17 (1978) 1305–1322.

[13] J.P. Browne, M. Strom, S.R. Martin, P.M. Bayley, The role of β-sheet interactions in domain stability, folding, and target recognition reactions of calmodulin, Biochemistry 36 (1997) 9550–9561.

[14] J.A. Schellman, Macromolecular binding, Biopolymers 14 (1975) 999–1018.

[15] S.R. Martin, L. Masino, P.M. Bayley, Enhancement by Mg^{2+} of domain specificity in Ca^{2+}-dependent interactions of calmodulin with target sequences, Protein Sci. 9 (2000) 2477–2488.

[16] H. Kuboniwa, N. Tjandra, S. Grzesiek, H. Ren, C.B. Klee, A. Bax, Solution structure of calcium-free calmodulin, Nat. Struct. Biol. 2 (1995) 768–776.

[17] M. Zhang, T. Tanaka, M. Ikura, Calcium-induced conformational transition revealed by the solution structure of apo-calmodulin, Nat. Struct. Biol. 2 (1995) 758–767.

[18] B.E. Finn, L. Evenäs, T. Drakenberg, J.P. Waltho, E. Thulin, S. Forsén, Calcium-induced structural changes and domain autonomy in calmodulin, Nat. Struct. Biol. 2 (1995) 777–783.

[19] H. Tjandra, H. Kuboniwa, H. Ren, A. Bax, Rotational dynamics of calcium-free calmodulin studied by ^{15}N-NMR relaxation measurements, Eur. J. Biochem. 230 (1995) 1014–1024.

[20] J.L. Urbauer, J.H. Short, L.K. Dow, A.J. Wand, Structural analysis of a novel interaction by calmodulin: high-affinity binding of a peptide in the absence of calcium, Biochemistry 34 (1995) 8099–8109.

[21] P.M. Bayley, Stopped-flow circular dichroism techniques: scope and limitations, Prog. Biophys. 37 (1981) 149–180.

[22] K. Kuwajima, A. Sakuraoka, S. Fueki, M. Yoneyama, S. Sugai, Folding of carp parvalbumin studied by equilibrium and kinetic circular dichroism spectra, Biochemistry 27 (1988) 7419–7428.

[23] H. Roder, M.C.R. Shastry, Methods for exploring early events in protein folding, Curr. Opin. Struct. Biol. 9 (1999) 620–626.

[24] M. Eigen, L. DeMaeyer, Theoretical basis of relaxation spectrometry, in: A. Weissberger, G.G. Hammes (Eds.), Techniques of Chemistry, vol. VI, 3rd ed., Wiley, New York, 1974, pp. 63–146.

[25] J. Hofrichter, Laser temperature-jump methods for studying folding dynamics, Methods Mol. Biol. 168 (2001) 159–191.

[26] M. Jacob, G. Holtermann, D. Perl, et al., Microsecond folding of the cold shock protein measured by a pressure-jump technique', Biochemistry 38 (1999) 2882–2891.

[27] T.N. Tsalkova, P.L. Privalov, Thermodynamic study of domain organisation in troponin C and calmodulin, J. Mol. Biol. 181 (1985) 533–544.

[28] R. Rigler, C.R. Rabl, T.M. Jovin, A temperature-jump apparatus for fluorescence measurements, Rev. Sci. Instrum. 45 (1974) 580–588.

[29] C.R. Rabl, Kinetik und Reaktionsmechanismus des biologischen Calcium-Indikators Arsenazo III. PhD Thesis, University of Konstanz, Germany, 1985.

[30] C.R. Rabl, Relaxationsmesstechnik, in: H.J. Rehm (Ed.), Technische Biochemie, Dechema Monographies, vol. 71, Verlag Chemie, Weinheim, 1973, pp. 187–205.

[31] E. Mihalyi, Numerical values of the absorbance of the aromatic amino acids in acid, neutral, and alkaline solutions, J. Chem. Eng. Data 13 (1968) 179–182.
[32] B.R. Sorensen, M.A. Shea, Interactions between domains of apo calmodulin alter calcium binding and stability, Biochemistry 37 (1998) 4244–4253.
[33] A.D. Robertson, K.P. Murphy, Protein structure and the energetics of protein stability, Chem. Rev. 97 (1997) 1251–1267.
[34] T. Schindler, F.X. Schmid, Thermodynamic properties of an extremely rapid protein folding reaction, Biochemistry 35 (1996) 16833–16842.
[35] S. Manyusa, D. Whitford, Defining folding and unfolding reactions of apocytochrome b_5 using equilibrium and kinetic fluorescence measurements, Biochemistry 38 (1999) 9533–9540.
[36] S.-I. Segawa, M. Sugihara, Characterisation of the transition state of lysozyme unfolding. I. Effect of protein–solvent interactions in the transition state, Biopolymers 23 (1984) 2472–2488.
[37] U. Mayor, C.M. Johnson, V. Daggett, A.R. Fersht, Protein folding and unfolding in microseconds to nanoseconds by experiment and simulation, Proc. Natl. Acad. Sci. USA 97 (2000) 13518–13522.
[38] M.A. Wilson, A.T. Brunger, The 1.0 Å crystal structure of Ca^{2+}-bound calmodulin: an analysis of disorder and implications for functionally relevant plasticity, J. Mol. Biol. 301 (2000) 1237–1256.
[39] G. Barbato, M. Ikura, L.E. Kay, R.W. Pastor, A. Bax, Backbone dynamics of calmodulin studied by ^{15}N relaxation using inverse detected two-dimensional NMR spectroscopy. The central helix is flexible, Biochemistry 31 (1992) 5269–5278.
[40] C.R. Rabl, High-resolution temperature-jump measurements using cooling correction, in: W.J. Gettins, E. Wyn-Jones (Eds.), Techniques and Applications of Fast Reactions in Solution, Reidel, Dordrecht, 1979, pp. 77–82.
[41] S.M. Coutts, D. Riesner, R. Römer, C.R. Rabl, G. Mass, Kinetics of conformational changes in $tRNA^{Phe}$ (yeast) as studied by the fluorescence of the Y-base and of formycin, Biophys. Chem. 3 (1975) 275–289.